Structural ability and electronic density of states in (001)- and (111)-oriented $(GaP)_1/(InP)_1$ strained-layer superlattices

1991 J. Phys.: Condens. Matter 3 6977

(http://iopscience.iop.org/0953-8984/3/36/003)

J. Phys.: Condens. Matter 3 (1991) 6977–6987. Printed in the UK

Structural stability and electronic density of states in (001)- and (111)-oriented $(GaP)_1/(InP)_1$ strained-layer superlattices

En-Ge Wang†‡§, Jian Zi‖ and Ding-Sheng Wang†‡

† Laboratory for Surface Physics, Institute of Physics, Academia Sinica, PO Box 603-91, Beijing 100080, People's Republic of China

‡ Center of Theoretical Physics, CCAST (World Laboratory), Beijing, People's Republic of China

§ International Center for Materials Physics, Academia Sinica, Shenyang 110015, People's Republic of China

‖ Department of Physics, Fudan University, Shanghai, People's Republic of China

Received 12 December 1990, in final form 15 April 1991

Abstract. The stability of (001)- and (111)-oriented $(GaP)_1/(InP)_1$ strained-layer superlattices (SLSs) is studied by the Keating model. The obtained deviations of the In–P and Ga–P bond lengths of the (001) stable superlattice structure from the constituent bulk lengths are −1.0% and 0.8%, respectively. A recursion method is used to calculate the bulk and surface electronic structures for both (001) and (111) $(GaP)_1/(InP)_1$ SLSs. It is found that the band gaps of the (001) and (111) structures, respectively, are smaller by 0.28 eV and 0.31 eV than the average of those of bulk InP and GaP. From the total-structural-energy and Fermi level calculation, we conclude that the strained-monolayer superlattice growth along the (001) direction is more stable than that along the (111) direction. A qualitative trend is proposed to elucidate the influence of strain on the electronic occupation in a strained-layer superlattice fabricated from III–V semiconductors, with the aid of two auxiliary systems. The localized states of a Si impurity in these systems are calculated.

1. Introduction

Over the past few decades, there has been a rapidly increasing effort in building very fine artificial superlattices. These multi-layer structures offer interesting opportunities in band-gap engineering, which have shown potential applications in optoelectronic devices. In 1985, Kuan *et al* [1] presented evidence for a long-range order in $Ga_{1-x}Al_xAs$ alloys grown on a GaAs substrate. At the same time, a neostructural order–disorder transition in the $Si_{1-x}Ge_x/Si(001)$ strained-layer superlattice (SLS) was reported [2].

The main theoretical studies [3–11] in this field were focused on the structural and electronic properties of superlattice systems. Ciraci and Batra [3] reported the stability analysis of short-period SiGe/Si and GaAs/AlAs systems using the self-consistent-field (SCF) pseudopotential method. They found that the neostructural phase transition lowers the total energy in the Si–Ge system only with a local minimum on the Born–Oppenheimer surface. A first-principles total-energy calculation [4] was performed to clarify the indirect and direct gap of $(GaAs)_n/(AlAs)_n$ ($n < 3$) superlattices. A detailed study on

0953-8984/91/366977 + 11 $03.50

Table 1. The Keating parameters α and β for bulk InP and GaP.

	α (eV Å^{-4})	β (eV Å^{-4})
InP	0.1560	0.0226
GaP	0.2017	0.0445

the stability and electronic structure of (001)-oriented $(GaAs)_1/(AlAs)_1$ superlattice was given by Wood *et al* [5]. From the semiquantitative description, they suggested that this system belongs to class III (unstable at $T = 0$ with respect to disordering, and unstable with respect to disproportion). The self-consistent pseudopotential calculation for electronic structure of the (001)-oriented $(InAs)_1/(AlAs)_1$ superlattice and for structural stability of the (111)-oriented $(InAs)_1/(AlAs)_1$ superlattice were presented by Taguchi and Ohno [6] and Magri and Calandra [7], respectively. Very recently, the stability [8] and electronic structure [9, 10] of GaP/InP systems have been studied by several groups. Because of the ability to cover a wide range of lattice mismatches and the potential for tailoring band gaps, it is necessary for us to carry out a more detailed investigation of the GaP/InP SLS.

In this paper, we present a further theoretical study on the structural, electronic and Si doping properties of (001)- and (111)-oriented $(GaP)_1/(InP)_1$ SLSs. The structural configurations of these systems are given within the Keating model [12, 13], which has been widely used to describe the elastic energy of covalent crystals with zinc-blende structure. The bulk and surface electronic structures of (001)- and (111)-oriented $(GaP)_1/(InP)_1$ SLSs are calculated using a recursion method [14–17]. In order to discuss the strain effect, some auxiliary systems are drawn into the calculations. Furthermore, the local environment of a Si impurity in the $(GaP)_1/(InP)_1$ SLS is presented for the first time.

Section 2 contains a brief description of the Keating model, and the stable parameters and strain tensors of a GaP/InP strained-monolayer superlattice are also obtained. In section 3 the bulk and surface electronic structures of these superlattices are presented. A comparison between (001)- and (111)-oriented systems is given. Some auxiliary models are set up to study the strain effect in section 4. Section 5 presents the local environment of the Si impurity and its influence on the electronic property of the GaP/InP SLS. The summary and discussion of our results are in section 6.

2. Structural stability and strain tensor

In this section, the structural properties of the $(GaP)_1/(InP)_1$ SLS is investigated by the Keating [12] model, which uses a short-range potential to describe tetravalent covalent bonds. The elastic energy of a structure with more than two kinds of atom in a unit cell described by the Keating potential [13] is

$$E = \sum \alpha_{(ss')}[X_{ss'} \cdot X_{ss'} - (b_s + b_{s'})^2]^2 + \sum \beta_{(ss's'')}[X_{ss'} \cdot X_{ss''} + \tfrac{1}{3}(b_s + b_{s'})(b_s + b_{s''})]^2 \tag{1}$$

where α and β are the bond-stretching and bond-bending force constants, respectively, which are taken from [18] and are listed in table 1. In equation (1), b_s is the covalent

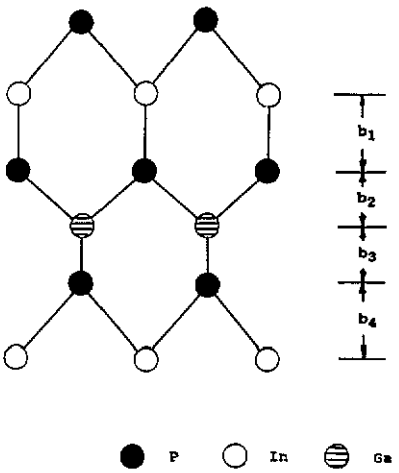

Figure 1. The side view of an ideal (001)-oriented $(GaP)_1/(InP)_1$ SLS, where b_i denotes the interplanar spacings.

radius of atom s, and $X_{ss'} = X_s - X_{s'}$ is the position vector between atom s and atom s'. The first sum is over all atoms and their four neighbours; the second sum is over all atoms and pairs of distinct neighbours.

In the present calculation, the bond-bending parameter for Ga–P–In in the interface region is assumed to be the arithmetic mean of those of the two materials. Our earlier work [19] on the Si/Ge superlattice has shown that the Keating parameters deduced by this method are reasonable with respect to the recent *ab initio* calculations given by Freyen *et al* [20].

The lattice constants for InP and GaP bulk materials are 5.8687 Å and 5.4512 Å, respectively. The side view of the (001)-oriented $(GaP)_1/(InP)_1$ SLS is drawn in figure 1. There are four atoms—one Ga, one In and two P—in a tetragonal unit cell. We assumed that the lattice mismatch between In–P and Ga–P layers is completely accommodated by the lattice strain. The interplanar distances of the stable (001)-oriented GaP/InP monolayer superlattice, which is referred to as model II, are given in table 2, where $a_\perp$ is the in-plane lattice constant. From this table, we can see that the deviations, −0.1% (In—P) and 0.8% (Ga—P), in the bond lengths are in good agreement with the results obtained by Nelson and Batra [8]. They proved that the In–P and Ga–P bond lengths in the stable $(GaP)_1/(InP)_1$ structure are within 1% of their bulk values by first-principles total-energy methods.

The superlattices experience a biaxial strain. The strain tensors can be obtained by equations

$$\varepsilon^i_{xx} = \varepsilon^i_{yy} = (a_\perp - a_i)/a_i \tag{2}$$

and

$$\varepsilon^i_{zz} = (a_\parallel - a_i)/a_i \tag{3}$$

where i is InP or GaP, and a_i is the lattice constant of the bulk material i. Table 3 shows the calculated results. It is easy to see that the InP sublattice is expanded in the z-axis growth direction and contracted in the x–y plane, and the opposite process happens in the GaP sublattice of the (001)-oriented $(GaP)_1/(InP)_1$ SLS.

Table 2. Characteristics of stable (001)-oriented $(GaP)_1/(InP)_1$ SLS determined by the Keating potential, referring to model II, and two auxiliary superlattices referring to models I and III, respectively.

	Value for the following models		
	I	II	III
$a_\perp$ (Å)	5.6086	5.6086	5.6600
$a_\parallel$ (Å)	5.7391	5.7292	5.6600
$b_1 = b_4$ (Å)	1.5892	1.5475	1.4150
$b_2 = b_3$ (Å)	1.2804	1.3171	1.4150
Bond length			
In–P	2.5412	2.5153	2.4509
Ga–P	2.3604	2.3805	2.4509
Deviation in the bond length from the bulk values (%)			
In–P	0	−1.0	−3.6
Ga–P	0	0.8	3.8

Table 3. Strain tensor for the (001)-oriented $(GaP)_1/(InP)_1$ superlattice models described in table 2.

	Value for the following models		
	I	II	III
	GaP		
$\varepsilon_{xx} = \varepsilon_{yy}$ (%)	2.9	2.9	3.8
ε_{zz} (%)	−6.0	−3.4	3.8
	InP		
$\varepsilon_{xx} = \varepsilon_{yy}$ (%)	−4.4	−4.4	−3.6
ε_{zz} (%)	8.3	5.5	−3.6

3. Bulk and surface electronic structures

A recursion method [14] has been used to calculate the electronic structures of (001)- and (111)-oriented $(GaP)_1/(InP)_1$ SLSs. The validity of the procedure developed for the semiconductor superlattice has been checked by comparison with the self-consistent full-potential linearized augmented-plane-wave (FLAPW) band calculation in our earlier papers [15–17]. It is especially suitable for discussing the local electronic structure of imperfect regions, such as the surface, the interface and point defects, where the periodic boundary condition breaks down in the superlattice. In this calculation, the cluster containing about 10000 atoms is taken as an imitation of a real crystal, and the recurrence chain length is selected as $L = 30$ by checking the convergence through calculations truncated at different maximum L-values.

The total densities of states (TDOSs) of (001)- and (111)-oriented stable $(GaP)_1/(InP)_1$ SLSs, corresponding to the full and broken curves, respectively, are given in figure 2(*a*). The structural parameters of the (111)-oriented $(GaP)_1/(InP)_1$ SLS are taken from

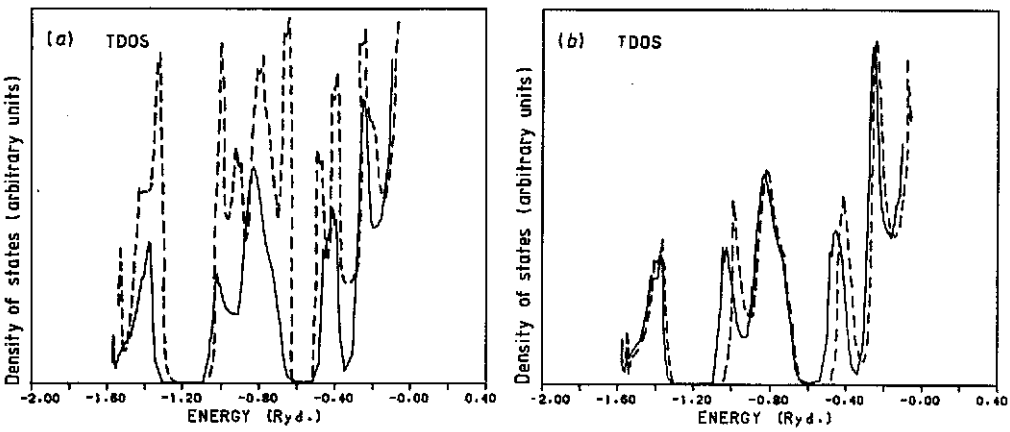

Figure 2. (*a*) TDOSs of stable (001)-oriented (——) and (111)-oriented (– – –) $(GaP)_1/(InP)_1$ SLSs determined by the Keating model and (*b*) TDOSs of bulk InP (——) and GaP (– – –).

[9] and [10]. By comparison with those of InP (full curve) and GaP (broken curve), in figure 2(*b*), we find that the TDOS shape of the (001)-oriented GaP/InP strained-monolayer superlattice is very similar to that of their bulk materials. The calculated band gaps are 1.91 eV for the (001)-oriented structure and 1.88 eV for the (111)-oriented structure, which are smaller by 0.28 eV and 0.31 eV than the average of the gaps of bulk InP (1.48 eV) and GaP (2.91 eV) materials, respectively. The result for the (111)-oriented $(GaP)_1/(InP)_1$ SLS coincides fairly well with a recent first-principles all-electron band-structure calculation (0.33 eV) [9]. Experimentally, the reduced band gap has been measured as 0.27 eV by photoluminescence [21, 22].

The Fermi levels of the (001)- and (111)-oriented $(GaP)_1/(InP)_1$ systems are -0.570 Ryd and -0.560 Ryd, respectively, where the zero of the energy scale is defined at an infinite distance. This suggests that the GaP/InP strained-monolayer superlattice growth along the (001) direction is more stable than that along the (111) direction.

A further discussion about local densities of states (LDOSs) and partial densities of states (PDOSs) of different atoms gives us a detailed description of the electronic structures of the $(GaP)_1/(InP)_1$ SLS. In the following, the z axis for the (001) structure is along (001), and the Z' axis along (111) for the (111) structure. From figures 3 and 4, we find that the shape of $P_{z'}$ partial wave is significantly different from that of $P_{x'}$ (or $P_{y'}$) partial wave in the (111)-oriented structure, while they are almost the same in the (001)-oriented structure. It is clear that the splitting of p states is the basic reason why the TDOS of the (111)-oriented $(GaP)_1/(InP)_1$ SLS is not similar to that of the constituent materials. The first TDOS peak of this SLS (in the energy region between -1.30 and -1.40 Ryd; see figure 2(*a*)) is mainly contributed by the S state, the second (between -0.94 and -1.04 Ryd) by the S state of the group III atom and $P_{z'}$ state of the group V atom, the third (between -0.86 and -0.94 Ryd) by the $P_{x'}$ and $P_{y'}$ states of the P atom, the fourth (between -0.70 and -0.86 Ryd) by the P state, and the peak at the top of valence band by the $P_{z'}$ state of the group V atom and by the $P_{x'}$ ($P_{y'}$) state of the group III atom. The situation for the (001)-oriented $(GaP)_1/(InP)_1$ SLS is simpler, where the states of highest valence band originate from the 5P level and the states at the bottom of conduction band from the 3S level.

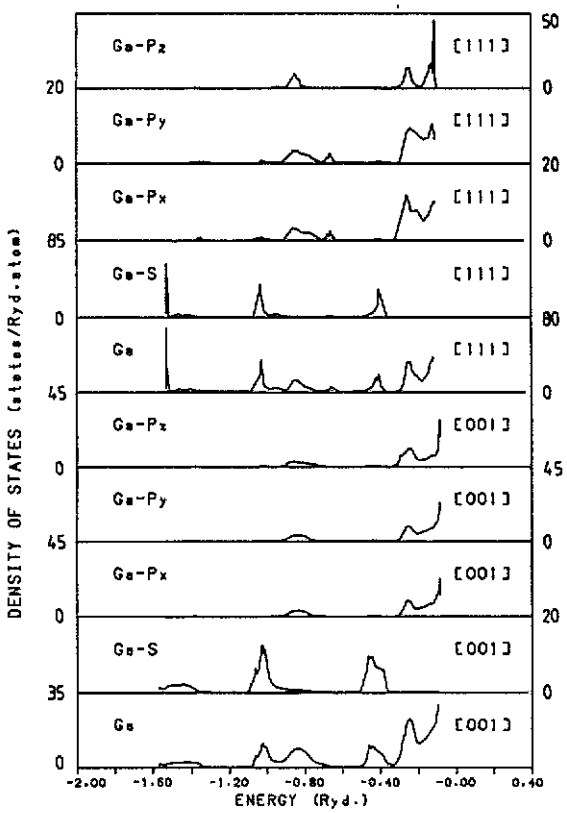

Figure 3. LDOSs and PDOSs of a Ga atom in (001)- and (111)-oriented $(GaP)_1/(InP)_1$ SLSs, where S and P_j $(j = x, y, z)$ refer to S and P orbitals, respectively.

Because of the existence of the broken bonds on the surface atoms, this will lead to a redistribution of the charge density. Figures 5(*a*) and (*b*) show the DOSs of a (001) surface In or P atom in (001)-oriented $(GaP)_1/(InP)_1$ SLs, respectively. The P_x (P_y) states on a group III surface atom become unbonding states (see figure 5(*a*)). There is SP_z mixed dangling bond, which is oriented perpendicular to the surface, and a P_x–P_y mixed bridge bond, oriented along the [110] direction, which forms $SP_z + P_x$–P_y dehybridization.

A similar dehybridization is found on a (111) surface atom in the (111)-oriented $(GaP)_1/(InP)_1$ SLS. However, it should be noted that the $P_{z'}$ level of a (111) surface P atom shifts more towards the Fermi energy E_F than do the $P_{x'}$ and $P_{y'}$ levels, which is different from the case of a (001) surface P atom in (001)-oriented $(GaP)_1/(InP)_1$ SLS (see figure 5(*b*)). This is due to the different coordinates used for the (001) and (111) systems. The higher occupied valence band of the P atom is about 17% wider than its bulk case. There are some surface states in the forbidden gap, which will make the band structure somewhat bent in the surface region.

4. Strain influence on electronic occupancy

In order to elucidate the stability of the above (001)- and (111)-oriented $(GaP)_1/(InP)_1$ SLSs determined by the Keating model, and to discuss the influence of strain on their electronic structures, there are two auxiliary superlattices taken into account. One is

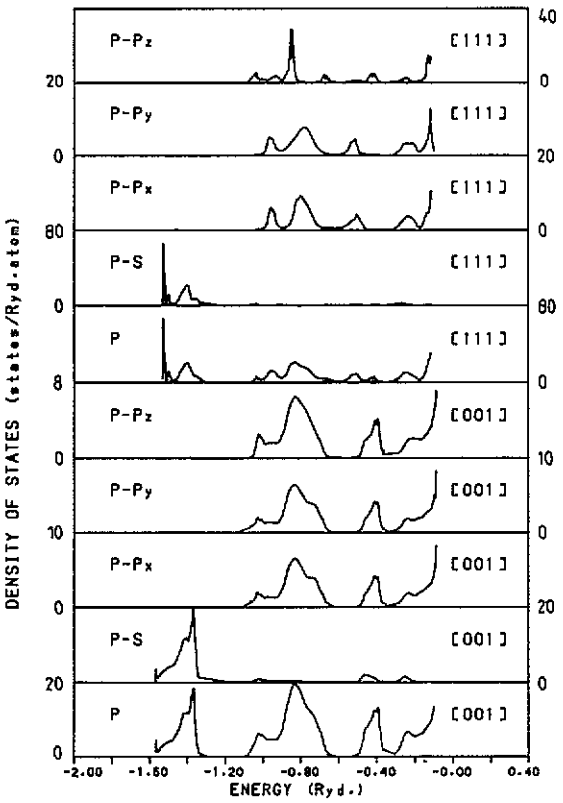

Figure 4. LDOSs and PDOSs of a P atom in (001)- and (111)-oriented $(GaP)_1/(InP)_1$ SLSs.

called model I, in which the In—P and Ga—P bond lengths are the same as those of the constituent bulk values, respectively. The other, model III, is an ideal zincblende structure, where all the bond lengths between two different nearest neighbours are equal to the average of bulk InP and GaP bond lengths. Their detailed characteristics are given in table 2.

Although there is no deviation in the bond lengths from their constituent bulk values for the $(GaP)_1/(InP)_1$ superlattice given as model I, the strain tensors are not equal to zero (see table 3). This is due to the change in unit-cell volume of this system. In model I, the InP sublattice is expanded in the (001) growth direction and contracted in the x–y plane. For the GaP sublattice we have the opposite situation. Different from models I and II, the GaP and InP sublattices in model III are simultaneously expanded or contracted in x, y and z directions. The Fermi levels in models I and III are -4.73 Ryd and -4.54 Ryd, respectively, which are higher than that of the stable (001)- and (111)-oriented $(GaP)_1/(InP)_1$ SLSs.

By integrating the local electronic density of states of an atom up to the Fermi level, we have obtained the electronic occupancy on each site. The results for the (001)-oriented $(Gap)_1/(InP)_1$ stable structure are given in table 4. It is clearly shown that In—P is more ionic than Ga—P, which will lead to a small charge transfer in the interface region.

As a key factor in investigating the influence of the strain on the electronic properties of GaP/InP systems, the charge distribution in the three models is calculated and given in figure 6. From table 3, we see that the Ga—P and In—P bond lengths become longer

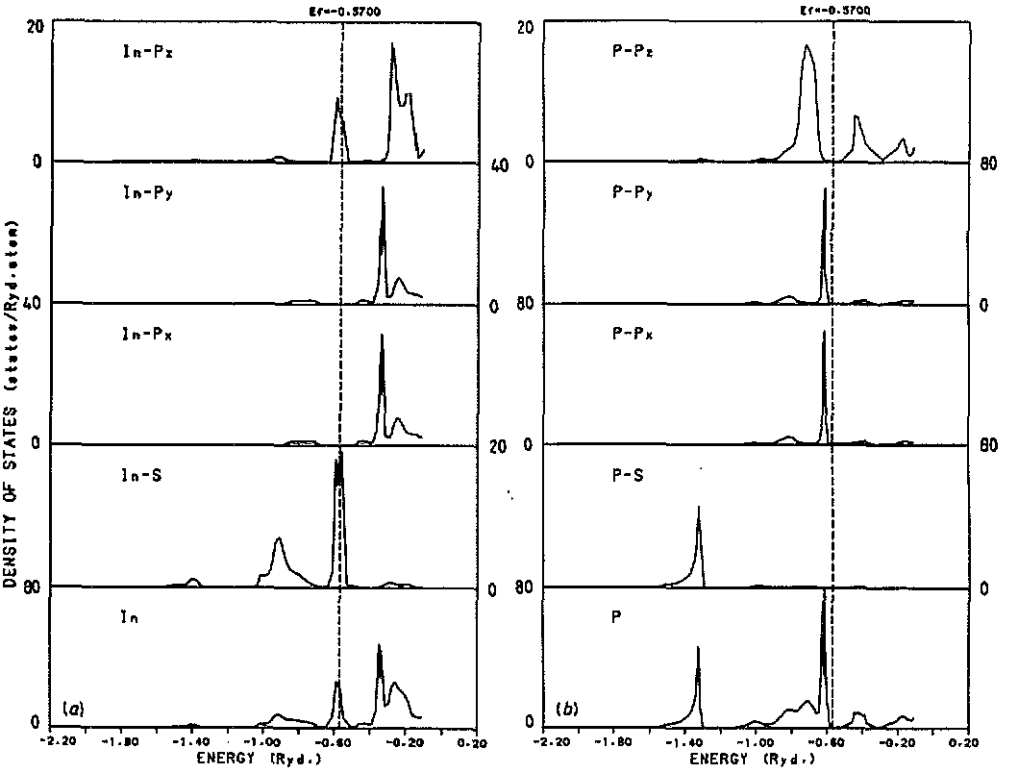

Figure 5. *LDOSS and PDOSS of a (001) surface atom in (001)-oriented $(GaP)_1/(InP)_1$ SLSs.*

Table 4. Electronic occupancies and valences in parentheses of Ga, In and P atoms in the stable (001)-oriented $(GaP)_1/(InP)_1$ SLS.

	s	p_x	p_y	p_z	Total
Ga	1.19	0.50	0.50	0.47	2.66 (+0.34)
In	1.09	0.43	0.43	0.40	2.35 (+0.65)
P	1.76	1.24	1.24	1.23	5.47 (−0.47)

and shorter as models go from I to III, respectively. That is to say the deviation in the bond lengths of these superlattice systems from the bond lengths of their bulks becomes larger in the order model I → model II → model III. The results drawn in figure 6 show that there will be more electrons on a Ga atom and fewer in an In atom with increasing bond length strain. Because the increase in the number of electrons in a Ga atom is more than the loss on an In atom, the electronic occupancy on an anion decreases at the same time. This qualitative trend may hold true in other SLSs fabricated from III–V semiconductors.

5. Localized states induced by the Si impurity

The doping of semiconducting materials is a basic step in the fabrication of electronic and optoelectronic devices. There have been quite a number of theoretical and experimental

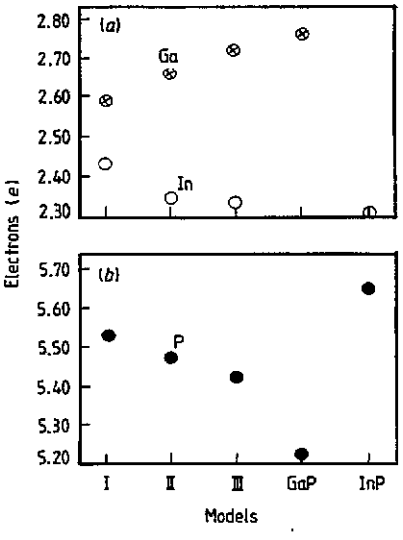

Figure 6. Electronic occupancy on an atom in several superlattice models and bulk materials.

contributions on the influence of different impurities on the electronic properties of the GaAs/AlAs superlattice [15, 23–27]. However, the problem in the GaP/InP SLS has scarcely been studied up to now.

The electronic structure of the (001)-oriented $(GaP)_1/(InP)_1$ SLS with a Si impurity is calculated in order to describe the local environment around the defect. Only some projected densities of states, e.g. the LDOSs of an impurity and its neighbours when a Si is substituted for an In atom, are shown in figure 7. First, we find that the Si-related impurity level in the (001)-oriented $(GaP)_1/(InP)_1$ SLS is located at 0.06 eV below the bottom of the conduction band. Because of the existence of the impurity, the higher occupied valence band edge width of a neighbour P atom is 8.9% wider than that of a P atom far from the Si dopant. The localized state is at $E_c - 0.09$ eV for Si substituting for a Ga atom, which is close to the experimental result $E_c - 0.083$ eV in bulk GaP [28].

Furthermore, the valence of the Si impurity is calculated to discuss its influence on the electronic properties of the GaP/InP SLS in some detail. It is found that the valences of Si on P, Ga and In sites are −0.535, +0.655 and +0.645, respectively. The results reflect the fact that the Si dopant is a negative centre when Si substitutes for a group V atom, and a positive centre when it substitutes for a group III atom. Therefore, the influence of the impurity on the electronic properties of the (001)-oriented $(GaP)_1/(InP)_1$ SLS can be explained in terms of an added charge owing to the presence of the Si atom.

6. Conclusion

The stability of the $(GaP)_1/(InP)_1$ SLS has been investigated by the Keating model. The determined structural parameters of the (001)-oriented GaP/InP strained-monolayer superlattice show that the deviation in the bond lengths from their bulk bond lengths is within 1%, which coincides with first-principles total-energy results [8]. From the calculation of the total structural energy and Fermi level, we find that the (001)-oriented SLS is more stable than the (111)-oriented SLS.

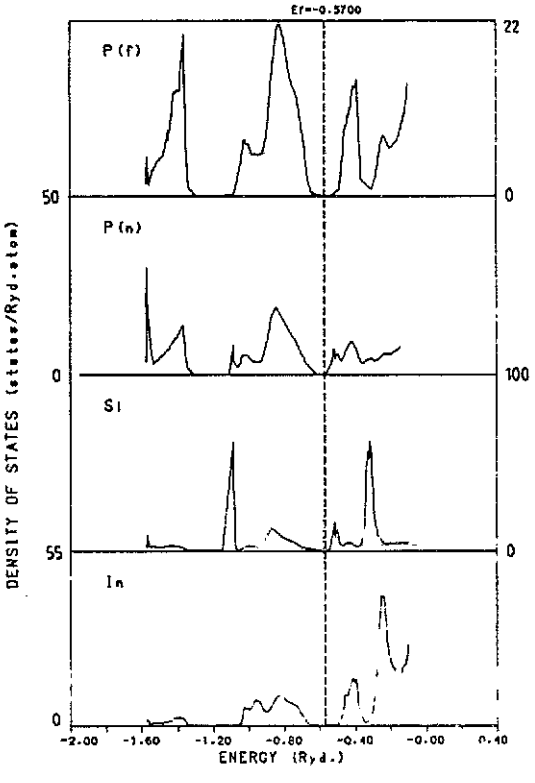

Figure 7. Influence of the impurity on the electronic structures of the (001)-oriented $(GaP)_1/(InP)_1$ SLS when Si is substituted for In, where the symbols (n) and (f) represent a P atom near to and far from the dopant, respectively. The LDOS of a normal In atom serves as reference.

A recursion method has been used to calculate the bulk and surface electronic structures of (001)- and (111)-oriented $(GaP)_1/(InP)_1$ SLSs, taking into account about 10000 atoms in the adopted cluster. We find that the band gaps of the (001) and (111) SLSs are smaller by 0.28 eV and 0.31 eV than the average of those of the InP (1.48 eV) and GaP (2.91 eV) bulk materials, respectively. The FLAPW result for the (111)-oriented $(GaP)_1/(InP)_1$ SLS is 0.33 eV [9]. The dehybridization on the (001) and (111) surfaces of the SLS is found. Two auxiliary superlattices are taken into account to elucidate the stability of the $(GaP)_1/(InP)_1$ SLS determined by the Keating model. A general qualitative trend is proposed to discuss the influence of the strain on the electronic occupancy in a SLS fabricated from III–V semiconductors.

Finally, the Si dopant property in the (001)-oriented $(GaP)_1/(InP)_1$ SLS has been described for the first time. The impurity-related localized states are calculated. Further study of the doping influence on the electronic properties of this system is of interest.

Acknowledgments

One of the authors (EGW) would like to acknowledge Dr Huaiyu Wang for assistance with the calculation, Professor Lianke Dong for his clear scientific discussion, and Ms Xiaowei Wang for her enthusiasm and support during his stay at the International Center for Materials Physics (ICMP), Academia Sinica, Shenyang. The work was supported by the ICMP from grant no 91008.

References

[1] Kuan T S, Kuech T F, Wang W I and Wilkie E L 1985 *Phys. Rev. Lett.* **54** 20
[2] Ourmazd A and Bean J C 1985 *Phys. Rev. Lett.* **55** 765
[3] Ciraci S and Batra I P 1987 *Phys. Rev. Lett.* **58** 2114
[4] Oshiyama A and Saito M 1987 *Phys. Rev.* B **36** 6156
[5] Wood D M, Wei S-H and Zunger A 1988 *Phys. Rev.* B **37** 1342
[6] Taguchi A and Ohno T 1987 *Phys. Rev.* B **36** 1696; 1988 *Phys. Rev.* B **38** 2038
[7] Magri R and Calandra C 1989 *Phys. Rev.* B **40** 3896
[8] Nelson J S and Batra I P 1989 *Phys. Rev.* B **39** 3250
[9] Kurimoto T and Hamada N 1989 *Phys. Rev.* B **40** 3889
[10] Wang En-Ge 1991 *5th Int. Conf. on Superlattices and Microstructures (Berlin, August 1990)*
[11] Granato E, Kosterlitz J M and Ying S C 1989 *Phys. Rev.* B **39** 3185
[12] Keating P N 1966 *Phys. Rev.* **145** 637
[13] Zi Jian, Zhang Kaiming and Xie Xide 1990 *J. Phys.: Condens. Matter* **2** 2473
[14] Haydock R 1980 *Solid State Physics* vol 35 (New York: Academic) p 216
[15] Wang En-Ge, Zhang Li-Yuan and Wang Huai-Yu 1989 *J. Phys.: Condens. Matter* **1** 8065
[16] Wang En-Ge, Jin Wei-Min, Zhang Li-Yuan and Wang Huai-Yu 1990 *J. Phys.: Condens. Matter* **2** 4405
[17] Wang En-Ge, Zhang Li-Yuan and Wang Huai-Yu 1989 *Phys. Status Solidi* b **155** 587; 1990 *Phys. Status Solidi* b **158** 589
[18] Martin R M 1970 *Phys. Rev.* B **1** 4005
[19] Zi Jian, Zhang Kaiming and Xie Xide 1991 *Phys. Rev.* B **41** 12 862
[20] Froyen S, Wood D M and Zunger A 1987 *Phys. Rev.* B **36** 4547; 1988 *Phys. Rev.* B **37** 6893
[21] Onton A, Lorenz M R and Renter W 1971 *J. Appl. Phys.* **42** 3420
[22] Gomyo A, Suzuki T and Iijima S 1988 *Phys. Rev. Lett.* **60** 2645
[23] Bastard G 1981 *Phys. Rev.* B **24** 4714
[24] Chaudhuri S 1983 *Phys. Rev.* B **28** 4480
[25] Liu Zhen-Peng and Li T K 1985 *J. Phys. C: Solid State Phys.* **18** 691
[26] Masselink W T, Chang Y C and Morkoc H 1985 *Phys. Rev.* B **32** 5190
[27] Nelson J S, Fong C Y, Batra I P, Pickett W E and Klein B M 1988 *Phys. Rev.* B **37** 10 203
[28] Pantelides S T 1975 *Festkörperprobleme (Advances in Solid State Physics)* vol 15 (Braunschweig: Vieweg) p 149